

# Asymmetric tunneling through ordered molecular layers

Ilan Benjamin,<sup>a)</sup> Deborah Evans, and Abraham Nitzan

School of Chemistry, the Raymond and Beverly Sackler Faculty of Science, Tel Aviv University, Tel Aviv, 69978, Israel

(Received 25 June 1996; accepted 5 November 1996)

Electron tunneling through ordered molecular barriers is found to depend on the tunneling direction. In particular, the transmission probability of an electron incident in the normal direction on a 10 Å water layer strongly polarized in the tunneling direction is 4–5 orders of magnitude larger when it enters from the positive (hydrogen) face than from the negative (oxygen) face, in contrast to continuum dielectric model prediction. This emphasizes the importance of the discrete multidimensional nature of the barrier structure and suggests possible rectifying properties of such barriers, beyond the linear regime. © 1997 American Institute of Physics. [S0021-9606(97)51603-5]

## I. INTRODUCTION

Electron transfer processes between donor and acceptor molecules or between metal electrodes are three-dimensional phenomena often described using one 1-*d* models. In particular, calculation of the corresponding electronic coupling is often done within such models, using the rationale that the electron tunneling process is dominated by the 1-*d* path of least action. Also, we often resort to 1-*d* models because more realistic treatments of tunneling phenomena are notoriously difficult. However, recent calculations of tunneling in model multidimensional systems<sup>1–3</sup> show that 1-*d* approximations can lead to serious quantitative and qualitative errors.

For electron transfer in a host solvent, the importance of multidimensional aspects is intimately related to the host molecular structure. In a structureless dielectric continuum the shortest, i.e., linear, path between the donor and acceptor centers is indeed the main route for the tunneling process, and a 1-*d* calculation with possible corrections for zero-point energy effects along other directions may suffice. However, the tunneling through realistic molecular solvents is subjected to multiple scattering by the nuclear cores, and is not necessarily dominated by a single path. (Even if it were, this path, necessarily strongly winding, would be hard to find.)

The inherently 3-*d* nature of electron tunneling through water has recently been demonstrated using numerical simulations.<sup>3–5</sup> In these simulations the water is confined between two walls which represent metal electrodes, and the transmission coefficient for an electron through the water layer is evaluated numerically for static, equilibrium water configurations. It has been shown that the tunneling is very sensitive to the dimensionality of the system and to the water structure.<sup>3</sup> For example, a surface dipole layer results from the preferred attraction of the water oxygens to the metal walls and contributes to the reduction in the effective barrier to tunneling. This cannot be described by the continuum dielectric model.

In this Communication we report on numerical results which demonstrate another aspect of the effect of a barrier molecular structure on its transmission characteristics—the

strong asymmetry in the tunneling properties of a barrier constructed with orientationally ordered molecular layers. Technical details and our main results are presented next and possible implications are discussed in the last section.

## II. MODELS AND NUMERICAL RESULTS

Figures 1(a) and 1(b) compare two barriers made of static water layers confined in the *x* direction between two model metal electrodes separated by  $L=10$  Å. The potential  $V(x)$  shown is the *y*–*z* average of the 3-*d* potential experienced by an electron moving between the electrodes. The bare potential (in the absence of water) is taken a rectangular barrier,  $S(x)=h$  for  $-L/2 > x < L/2$  and  $S(x)=0$  for  $|x| > L/2$ , with  $h=5$  eV. Superimposed on it is the electron water interaction potential, taken here as a polarizable version<sup>5</sup> of the electron–water pseudopotential of Barnett *et al.*<sup>6</sup> Water configurations, taken static during the tunneling event, are prepared by running classical MD trajectories for the water confined between the two walls at 300 K, after ~100 ps of numerical annealing, using periodic boundary conditions in the *y* and *z* directions with period length 23.5 Å. The unit box contains 192 water molecules, corresponding to a density of 1 g/cc. The water-wall interaction is a superposition, for all O and H atoms of 3–9 potentials  $V_w = A/d^9 - B/d^3$ , where  $d$  is the distance from the wall and the parameters  $A$  and  $B$  are chosen to mimic the water–gold potential.<sup>7</sup> A flexible RWKM-2 potential<sup>8</sup> is used for the water–water interaction. In the resulting equilibrium configurations the water forms three molecular layers parallel to the walls with the oxygen ends of the monolayers adjacent to the walls oriented towards these walls. These configurations are, on the average, symmetric with respect to the center of the barrier as indicated by Fig. 1(a). The high potential peaks result from the strong repulsion of the electron from the core of the water oxygens. Figure 1(b) shows the similarly averaged potential obtained from oriented water structures which are prepared by repeating the MD runs in the presence of a strong electric field, 5 V/Å, in the negative *x* direction,<sup>9</sup> resulting in configurations where the water dipoles mostly point in this direction. The field is used here merely as a

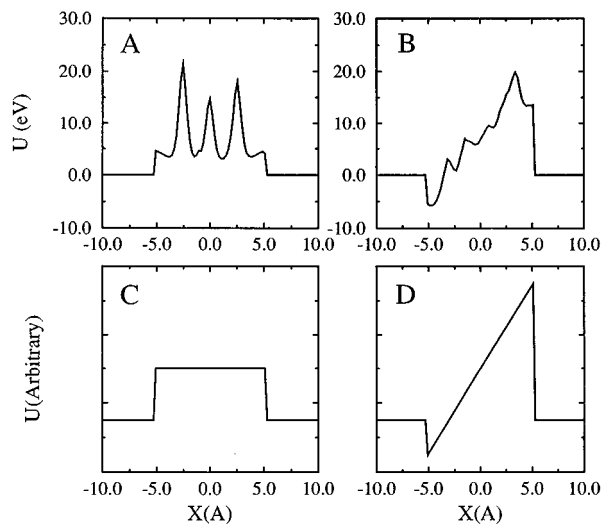


FIG. 1. (a) The  $y$ - $z$  average of the potential barrier experienced by an electron moving between two walls separated by a water layer; the model and the interaction potentials are described in the text. (b) Same as (a), with the water layer oriented by an electric field  $-5$  eV/Å. In both cases a rectangular barrier of height 5 eV is superimposed on the electron-water interaction. (c) and (d) Schematic views of the corresponding continuum dielectric models for the barrier.

numerical tool to orient the dipoles and does not directly affect the tunneling electron. In the corresponding continuum dielectric models the resulting potential barriers are effectively one-dimensional, given by Fig. 1(c) and 1(d). In particular, the dipolar ordering in Fig. 1(b) corresponds to a uniform polarization in the system, leading to the one-dimensional skewed barrier shown in Fig. 1(d). Microscopic reversibility implies that the transmission probability for an electron moving through the latter barrier does not depend on its direction:  $T_{R \rightarrow L} = T_{L \rightarrow R}$ , where  $T_{R \rightarrow L}$  and  $T_{L \rightarrow R}$  are the transmission probabilities for a particle coming from the right and from the left, respectively.

In reality, the multidimensional discrete molecular structure of the barrier changes this symmetry in an essential way. Figure 2 shows numerical results for the transmission prob-

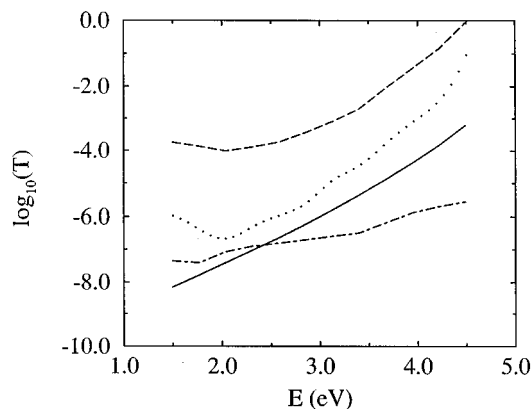


FIG. 2. Electron transmission probabilities between the two walls described in the text. Full line:  $T_{\text{vac}}$ , dotted line:  $T_w$ , dashed and dashed-dotted lines: water oriented by a field 5 eV/Å with tunneling direction opposite and identical to the orienting field, respectively.

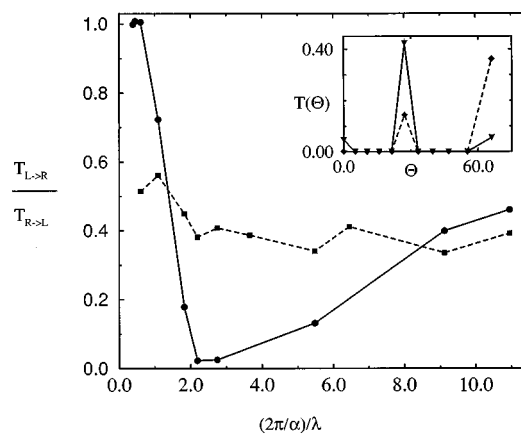


FIG. 3. The ratio between the total (integrated over all final directions) tunneling probabilities for an electron incident in the normal direction from the left and from the right on the barrier defined by Eqs. (1)–(2), plotted against the dimensionless parameter  $(\alpha\lambda)^{-1}$ , for the parameters given in the text. Solid line: barrier is periodic with period  $2\pi/\alpha$  in the  $y$  direction. Dashed line: average over results from three irregular barrier configurations (see text). The inset shows the normalized angular distributions of the transmission for a normally incident particle coming from the left (solid line) and from the right (dashed line), for the  $y$ -periodic case with  $2\pi/(\alpha\lambda) = 2.0$ .

ability vs electron energy for the 3- $d$  water structures that were used to generate Figs. 1(a) and 1(b). Shown are, as functions of the electron energy  $E$ , the transmission probabilities  $T_{\text{vac}}$  and  $T_w$ , for a bare gap and for a gap containing water, respectively, as well as  $T_{L \rightarrow R}$  and  $T_{R \rightarrow L}$  for gaps containing water ordered by a field 5 V/Å which is switched off during the tunneling itself. These transmission probabilities are for an electron incident normal to the barrier, and represent integrals over all transmitted directions. They were computed by real time propagation of the incident wave function on a grid, using the Chebyshev polynomial method<sup>10</sup> (see Ref. 3 for technical details). The simulated model accounts qualitatively for the substantial increase in the transmission probability when water replaces vacuum in the barrier.<sup>5</sup> The new striking observation is the huge effect of ordering in the water structure which results in  $T_{L \rightarrow R}/T_{R \rightarrow L} = 10^4 - 10^5$ , depending on electron energy. The barrier has become in a sense a strong rectifier due to the imposed molecular ordering. As discussed below, this reflects the marked difference between the angular dependence of the transmission probabilities for electrons traveling in opposite directions with respect to the barrier. We emphasize again that a continuum dielectric model of the barrier would yield  $T_{L \rightarrow R} = T_{R \rightarrow L}$  at all energies, even when the induced nuclear polarization associated with the ordering field is taken into account.

### III. DISCUSSION AND CONCLUSIONS

The observed asymmetry in the tunneling behavior is a direct and general consequence of the multidimensional asymmetric structure of the barrier. To demonstrate this within a relatively simple model we show in Fig. 3 the ratio  $T_{L \rightarrow R}/T_{R \rightarrow L}$  for plane waves  $\exp(ik_x x)$  incident from the left, and  $\exp(-ik_x x)$  incident from the right, on the 2- $d$  potential barrier

$$V(x,y) = S(x) + f_1(x)f_2(y), \quad (1)$$

where  $S(x)$  is the rectangular barrier defined above ( $h=5$  eV,  $L=10$  Å) and

$$f_1(x) = A \sin\left(\frac{\pi x}{L}\right), \quad f_2(y) = \frac{1 + \sin(\alpha y)}{2}, \quad (2)$$

where  $x$  is the tunneling direction. The second term in (1) represents the structure in the barrier potential: The function  $f_2(y)$ , with period  $2\pi/\alpha$ , mimics the discrete nature of the barrier while  $f_1(x)$  defines its asymmetry in the tunneling direction. Alternatively  $\alpha$  is replaced by a random function of  $y$ ,  $a(y)$ , distributed uniformly in the interval  $(\alpha/2, 3\alpha/2)$ , in order to mimic a disordered layer.  $T$ , the transmission probability summed over all final directions, is calculated by representing  $V(x,y)$  on a 2- $d$   $100 \times 50$  grid, with grid spacing  $\Delta_x = 0.21$  Å and  $\Delta_y = 0.5 - 1.0$  Å [depending on  $\alpha$  in Eq. (2)] and using the absorption boundary conditions Green's function method.<sup>11</sup> Figure 3 displays  $T_{L \rightarrow R}/T_{R \rightarrow L}$  vs the dimensionless parameter  $\eta = [2\pi/\alpha]/\lambda$ , where  $\lambda = 2\pi/(2mE)^{1/2}$  is the DeBroglie wavelength, for  $E = 4$  eV and  $A = 10$  eV. The periodic asymmetric barrier (solid line) shows a strong minimum at which  $T_{L \rightarrow R}/T_{R \rightarrow L} < 0.05$ , indicating the strong asymmetry of the tunneling behavior in the two directions. In the randomly ordered case (dotted line; computed with  $\Delta_y = 0.5$  Å) the tunneling probability shows a weaker dependence on  $\eta$ ,<sup>12</sup> but the asymmetry between the two tunneling directions remains considerable. Other choices for  $f_1(x)$  satisfying  $f_1(x) = -f_1(-x)$ , e.g.,  $f_1(x) = x/2L$ , yield similar results. Obviously, in the symmetric case,  $f_1(x) = f_1(-x)$ , the tunneling is symmetric:  $T_{L \rightarrow R} = T_{R \rightarrow L}$ .

Microscopic reversibility implies strict symmetry of the  $S$  matrix between incident and transmitted wave vectors, i.e.,  $S(k_i, k_t) = S(k_t, k_i)$ . Therefore the cumulative transmission probability  $T_c = \sum_{k_i} \sum_{k_t} |S(k_i, k_t)|^2$  does not depend on the incident direction. The probabilities displayed in Figs. 2 and 3 represent the partial sums  $\sum_{k_i} |S(k_i, k_t)|^2$  for  $k_i$  normal to the barrier, and their asymmetry results from the marked difference between the angular distribution of the transmission probabilities for particles coming from the left and from the right, as shown in the inset to Fig. 3. It should also be emphasized that while we have focused on electron tunneling, this asymmetry is not necessarily a quantum phenomenon. In fact, a similar qualitative effect is seen also when the incident energy is larger than the peak barrier energy, provided that orientational ordering exists in the barrier.

In order to observe the effect described above one should generate the necessary molecular order and maintain it in the absence of the ordering field during the electron transmission experiment. A possible way to do it is to orient dipolar molecules in a strong external electric field at a relatively high temperature, then to switch off the field after

freezing the orientational order by cooling the system. The transmission properties of such fields can be in principle studied by direct electron scattering experiments. It is of particular interest to consider the potential rectifying property of such films. Model molecular rectifiers, e.g., that suggested by Aviram and Ratner,<sup>13</sup> are usually associated with a particular electronic structure of a donor/acceptor system. Here the rectifying property is suggested by the observation that the angular distribution of transmission through ordered molecular layers may strongly depend on the tunneling direction. Note that, as in other rectifying devices, the Onsager relations imply strict symmetry in the linear response regime about equilibrium.<sup>14</sup> However, the fact that for finite potential bias the current is dominated mainly by the transmission probability normal to the barrier should lead to asymmetry in the current-voltage dependence beyond the linear regime. The bias at which deviations from symmetry appear depends on the scattering processes which drive the electron gas toward equilibrium, and cannot be determined in the context of the present work.

## ACKNOWLEDGMENTS

This paper was supported in part by the U.S.–Israel BSF and by the Israel Ministry of Science. We thank H. Tal Ezer, J. Imry, and T. Seidman for useful discussions.

<sup>a)</sup>Permanent address: Department of Chemistry, University of California, Santa Cruz, CA 95064.

<sup>1</sup>See, e.g., B. Das and J. Mahanty, Phys. Rev. B **36**, 898 (1987); P. Bowcock and R. Gregory, Phys. Rev. D **44**, 1774 (1991); M. Razavy and V. J. Cote, Phys. Rev. A **49**, 2266 (1994), and references therein.

<sup>2</sup>V. I. Goldanskii, Ann. Rev. Phys. Chem. **27**, 85 (1976); G. C. Schatz, B. Amae, and J. N. L. Connor, J. Chem. Phys. **93**, 5544 (1990); R. Baer, Y. Zeiri, and R. Kosloff (unpublished).

<sup>3</sup>A. Mosyak and A. Nitzan, J. Chem. Phys. **104**, 1549 (1996).

<sup>4</sup>W. Shmickler, Surf. Sci. **335**, 416 (1995).

<sup>5</sup>A. Mosyak, P. Graf, I. Benjamin, and A. Nitzan, J. Chem. Phys. (in press).

<sup>6</sup>R. N. Barnett, U. Landman, and C. L. Cleveland, J. Chem. Phys. **88**, 4420 (1988).

<sup>7</sup>J. Hautman, J. W. Halley, and Y.-J. Rhee, J. Chem. Phys. **91**, 467 (1989).

<sup>8</sup>J. R. Reimers and R. O. Watts, Chem. Phys. **85**, 83 (1984).

<sup>9</sup>This field is of the order of the strongest field used in recent MD simulations [X. Xia and M. L. Berkowitz, Phys. Rev. Lett. **74**, 3193 (1995)] and is somewhat higher than the strongest field used in recent experiments [M. F. Toney, J. N. Howard, J. Richer, G. L. Borges, J. G. Gordon, O. R. Melroy, D. G. Wlesler, D. Yee, and L. B. Sorensen, Nature **368**, 444 (1994)]. Weaker fields will be needed for substances without the strong H-bond structure and at lower temperature.

<sup>10</sup>H. Tal Ezer and R. Kosloff, J. Chem. Phys. **81**, 3967 (1984).

<sup>11</sup>T. Seidman and W. H. Miller, J. Chem. Phys. **96**, 4412 (1992); **97**, 2499 (1992).

<sup>12</sup>The dotted line in Fig. 2 corresponds to an average over three random barrier configurations. The irregular behavior is expected to smooth out with more configurational averaging.

<sup>13</sup>A. Aviram and M. A. Ratner, Chem. Phys. Lett. **29**, 277 (1974).

<sup>14</sup>See, e.g., Y. Imry, in *Directions in Condensed Matter Physics*, edited by G. Grinstein and G. Mazenko (World Scientific, Singapore, 1986), p. 101.